Oxygen exchange between an O_2 adsorbate and CaO surfaces

Yasunori Yanagisawa, Shinichi Yamabe, Keiko Matsumura, and Ryoitiro Huzimura
Department of Physics, Nara University of Education, Takabatake-cho, Nara 630, Japan
(Received 7 December 1992; revised manuscript received 22 March 1993)

Thermal desorption of $^{16}O^{18}O$ and $^{16}O_2$ gases after $^{18}O_2$ gas adsorption on CaO has been observed in the temperature range 120–1100 K, indicating that single and double oxygen exchange reactions occur on CaO surfaces even at low temperatures. To elucidate the mechanism of the two reactions, an *ab initio* molecular-orbital calculation is performed by use of a Ca_7O_5-O_2 cluster model. The reactions are found to take place via O_3 and O_4 intermediates, respectively. Their selectivity is ascribed to the absence or to the presence of molecular oxygen ion pairs at a kink site on a single-atom stepped (111) surface before $^{18}O_2$ adsorption.
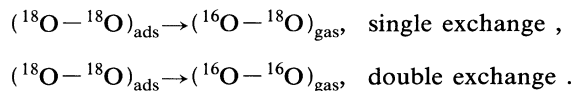
CaO is an active material in reactions such as pollutant removal in coal combustion[1] and catalysis of oxidative coupling of methane.[2] However, little is known about the interaction of oxygen molecules with CaO surfaces, since most investigations have been performed so far under practical conditions of gas-surface interactions, e.g., at rather high gas pressures.[3] Here, we report the observation of oxygen isotope exchange between the O_2 adsorbate and lattice oxygens of CaO surfaces and a plausible mechanism of bond interchange in this reaction. This is an attempt to analyze the O_2 exchange reaction on oxide surfaces of thermal energy level.

A CaO powder of "Specpure" grade (99.9992%) from Johnson Matthey Chem. Ltd. was preheated at 1150 K for several hours in a quartz tube (4 mm in diameter) attached to a vacuum system. The base pressure was 7×10^{-9} Torr. The sample was exposed to $^{18}O_2$ gas (98% ^{18}O) at 110 K for a desired time with the exposure range of 10^2–5×10^3 L ($1\ L = 1 \times 10^{-6}$ Torr s) in the dark, and thermally stimulated desorption (TSD) measurements were carried out using a quadrupole mass spectrometer from 110 to 300 K and from 300 to 1100 K with a heating rate 0.5 K/s.

After several cycles of exposure and TSD, reproducible thermal desorption (TD) curves were obtained, and typical TD curves after 2000-L exposure of $^{18}O_2$ are shown in Fig. 1. Below room temperature (RT), TD peaks of $^{18}O_2$ are observed at the peak temperatures (T_p's) 145 (peak α), 180 (β_1), and 220 K (β_2), with a shoulder at about 250 K (β_3). In addition, we find both $^{16}O^{18}O$ and $^{16}O_2$ TD peaks at 220 K with shoulders at 180 and 250 K. Thus peak α consists of only $^{18}O_2$, indicating that no oxygen isotope exchange occurred for this peak (physisorption only). Other TD peaks of $^{18}O_2$ are accompanied by TD's of $^{16}O^{18}O$ and $^{16}O_2$ (although only of minor intensity) at the same T_p's. A remarkable thermal exchange reaction of adsorbed O_2 with lattice oxygen takes place on CaO surfaces even at low temperatures below RT. Such exchanges have been previously observed only on the activated (UV-irradiated) MgO powders.[4] Above RT, TD peaks are observed at 390–570 and 930 K, as shown in Fig. 1(b). Peak β_4 at about 390 K consists of $^{18}O_2$, $^{16}O^{18}O$, and $^{16}O_2$, and peak β_5 at about 480–570 K mainly of $^{16}O^{18}O$ and $^{16}O_2$ with a small amount of $^{18}O_2$. The T_p of peak β_5 seems to shift toward lower temperature

(from 570 to 480 K) with the increase of molecular mass $^{16}O_2 \rightarrow {}^{16}O^{18}O \rightarrow {}^{18}O_2$. Peak γ at 930 K consists of only $^{16}O_2$. The same TD features were also observed after $^{18}O_2$ exposure at RT. No T_p changes of each TD peak were observed in the exposure range of 10^2–5×10^3 L. All of the TD peak heights increased linearly with the exposure and were not fully saturated even at a relatively high exposure (~ 5000 L), and peak γ began to dominate at higher exposures. TD's of CO and CO_2 were not observed in the temperature range examined, indicating negligible carbon contamination. The oxygen-isotope exchange with lattice oxygens is affected considerably by residual surface hydroxyls under the moderate outgassing conditions.[3] Based on IR measurements, Coluccia *et al.* reported that no surface H or OH group of CaO powders was detected after the high-temperature (~ 1100 K) and high-vacuum ($< 7 \times 10^{-7}$ Torr) pretreatments.[5] Thus the hydrogen concentration is thought to be very low in the present CaO powders.

In order to examine the exchange ratio (R), the TD intensity was estimated from the area under the respective TD peaks. The deconvolution of the overlapped TD peaks into two to four peaks was performed by tentatively assuming a Gauss-type TSD line shape, as shown in Fig. 1. $R(^{16}O^{18}O)$ and $R(^{16}O_2)$ are defined respectively as the ratios of $^{16}O^{18}O$ and $^{16}O_2$ TD intensities to the sum of intensities of $^{18}O_2$, $^{16}O^{18}O$, and $^{16}O_2$ TD peaks. $R(^{16}O^{18}O)$ or $R(^{16}O_2)$ for each TD peak was almost independent of $^{18}O_2$ exposures. $R(^{16}O^{18}O) = 0.35 \pm 0.03$ and $R(^{16}O_2) \approx 0.05$ for three low-temperature peaks β_1, β_2, and β_3. $R(^{16}O^{18}O)$ for peaks β_4 and β_5 is 0.44 ± 0.02, while $R(^{16}O_2)$ for these peaks gradually increases from 0.2 to 0.5 with TD temperature. $R(^{16}O_2)$ for peak γ is 1.0. Thus, we have found two reactions:

$$(^{18}O - {}^{18}O)_{\text{ads}} \rightarrow (^{16}O - {}^{18}O)_{\text{gas}}, \quad \text{single exchange},$$

$$(^{18}O - {}^{18}O)_{\text{ads}} \rightarrow (^{16}O - {}^{16}O)_{\text{gas}}, \quad \text{double exchange}.$$

A cluster-model geometry optimization with the *ab initio* molecular orbital is performed. Since we prefer to use as large a cluster as possible, at the cost of higher accuracy in computational method, we use the RHF/STO-3G method implemented in the GAUSSIAN 90 (G90) program.[6] Two coordinatively unsaturated oxygen atoms may be necessary for a site for the double exchange.
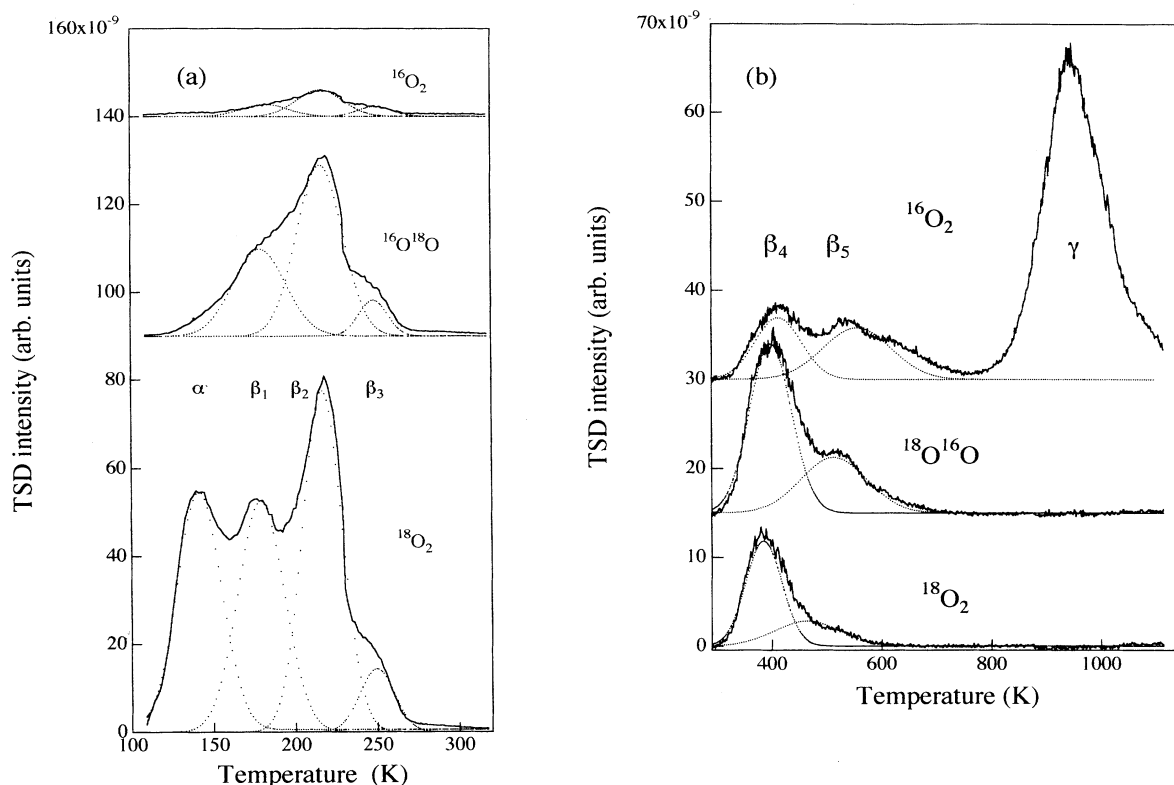
FIG. 1. TD of $^{18}O_2$, $^{16}O^{18}O$, and $^{16}O^2$ gases after 2000-L exposure to $^{18}O_2$ at 100 K of CaO powder baked at 1150 K, in the temperature range (a) 100–300 and (b) 300–1100 K. Dotted lines denote tentatively separated TD peaks by assuming a Gauss-type TSD line shape.

Hence we select a step site in direction ⟨101⟩ with an oxygen kink on the (111) cation planes (see Fig. 2) as a Ca_7O_5 cluster [see Fig. 3(i), state a]. Two more Ca atoms are needed to express reasonably the (111) cation plane on which the oxygen kink lies. Since the geometry optimization including the Madelung potential (MP) is not available in G90, we face the problem of the evaluation of the potential effect and selection of the charge of the cluster[7] and CaO may be considered almost as purely ionic as MgO.[8] Then the full system should be expressed as ([point-charge (PC) array]$^{4-}$+$(Ca_7O_5)^{4+}$) $\cdots$ O_2 if the reaction should occur within the neutral condition. However, to examine in G90 the system with which an O_2 molecule is interacting, we may approximate this as ([PC array]$^{4-}$+Ca_2^{4+} +$(Ca_5O_5)^0$) $\cdots$ O_2^0 ≈([PC array]^0Ca_2^0+$(Ca_5O_5)^0$) $\cdots$ O_2^0. Hence we calculate the total energy (E_t) or optimal structures in G90 without a PC array for Ca_7O_5+O_2 (with 180 electrons).

Two additional calculations were made in order to test the reliability of STO-3G geometries and energies. First, an optimization of the most important intermediate [state D in Fig. 3(ii)] is carried out with RHF/LANL1DZ+basis set, in which Ca inner-shell electrons are treated by the effective core potential, and valence electrons are treated by the double-zeta basis set (LANL1DZ).[9] For the oxygen anions, a set of diffuse sp orbital ($+$) is added to LANL1DZ.[10] The MP is not taken into account at this geometry optimization. Second, the 60-cation and 62-anion PC array is added to the Ca_7O_5 cluster to describe a kink site in Fig. 2. The aver-

aged charge values, ±1.30 are adopted, which are taken from the RHF/LANL1DZ+charge of the Ca_7O_5 cluster. These single-point energy calculations were made on several states [b, c, and d in Fig. 3(i), and B, C, D, and E
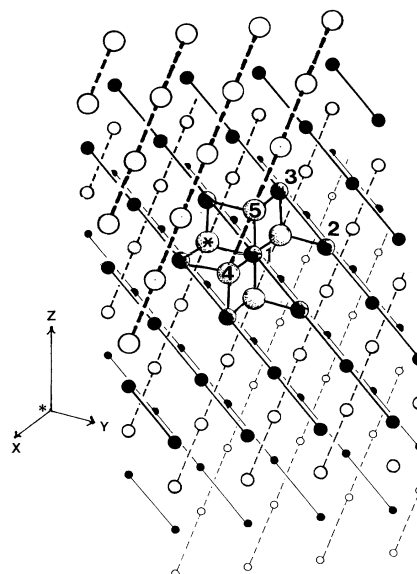

FIG. 2. The surface model with a step site on a (111) polar plane. The O(4) atom is located at the kink. The shaded-circle oxygen atom with the * sign is at the origin of Cartesian coordinates. 60-cation and 62-anion charges (±1.30) are located around the Ca_7O_5 cluster as an approximation of the Madelung potential.
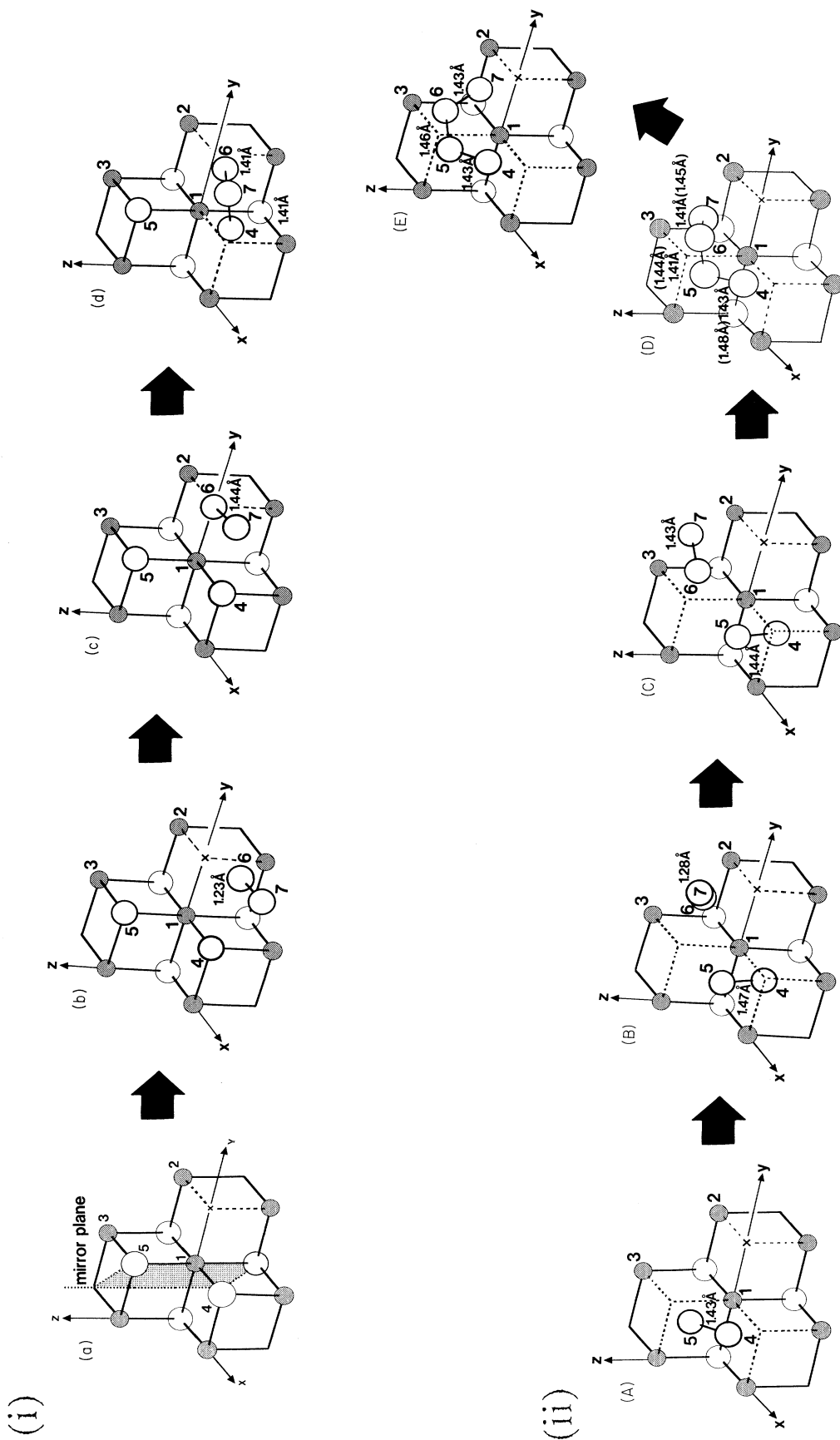
FIG. 3. Geometric changes of (i) the single and (ii) the double oxygen exchange reactions optimized partially with RHF/STO-3G. In (i), state a, all atoms are located at lattice points and only Ca-O distances (l) are optimized. In states b and c, positions of O(6) and O(7) and l are optimized. In state d, positions of O(6), O(7), and O(4) and l are optimized. The mirror plane of the Ca_7O_5 cluster is indicated as a shaded ($\bar{1}10$) plane. The point x stands for an oxygen vacancy. In (ii), state A, positions of O(4) and O(5) and l are optimized. In states B, C, D, and E, those of O(4), O(5), O(6), and O(7) and l are optimized. The geometry of state E is calculated under the C_s-symmetry restriction. For D, distances in parentheses are those obtained with RHF/LANL1DZ+.

in Fig. 3(ii)]. G90 installed at the CONVEX C-220 computer was used.

For the Ca_7O_5 kink model, two cases are considered. One is that two oxygen atoms at the kink, O(4) and O(5), are fixed at lattice points shown as state a in Fig. 3(i), and the other is that they form a molecular oxygen on the surface shown at A in Fig. 3(ii). This formation of the O_2^{2-} state at the cation vacancy in MgO was predicted by Freund.[11] The nearest-neighbor distance between Ca and O atoms is calculated to be 2.348 Å in state a and 2.387 Å in A, respectively, which may be in good agreement with the bulk data, 2.405 Å. The STO-3G (and LANL1DZ+) net charge on the O(4) [or O(5)] atom is -0.397 (and -1.354) at state a of Fig. 3(i) and -0.375 (and -0.691) at state A of Fig. 3(ii). As expected, the anionic character of each oxygen atom is decreased relative to that of the lattice oxygen through the molecular-type O(4)-O(5) bond formation.

The single exchange is examined in Fig. 3(i). When an adsorbed $^{18}O_2$ approaches the undistorted CaO surface of state a, it is trapped as state b. This trapping is physisorption, because the O(6)-O(7) bond elongation is small, 1.217 Å of free $O_2 \rightarrow 1.229$ Å in state b. If the one oxygen atom O(6) is captured at the oxygen vacant site (point x), the O(6)-O(7) bond is elongated to 1.443 Å to be bound tightly to the surface as state c. The next process is the linkage of O(7)-O(4) to bring about state d. Although locations of the three atoms O(6), O(7), and O(4) are determined independently, the C_s-symmetry structure of state d is obtained. The bridged geometry is the turning point of the single oxygen exchange. That is, if the O(6)-O(7) bond is cleaved in state d, state c' is arrived at to form the O(7)-O(4) molecule. States with primes are, hereafter, symmetric ones with respect to the mirror plane [see state a in Fig. 3(i)]. After the route, $c' \rightarrow b' \rightarrow a'$, it is possible for the half-exchanged O_2 molecule (i.e., ^{16}O-^{18}O) to desorb. Thus state d is the key intermediate for the single exchange. The STO-3G stabilizing energy at route $b \rightarrow c$ is -1.25 eV and that at $c \rightarrow d$ is -3.50 eV, which appears to be overestimated by the small basis set. These energies are obtained by the difference of the STO-3G E_t's.

The double exchange is examined in Fig. 3(ii). When an adsorbate $^{18}O_2$ approaches the distorted CaO surface of state A, it is trapped along the principal axis of the equilateral triangle composed of Ca(1), Ca(2), and Ca(3) to form state B. This trapping is physisorption with the $^{18}O(6)$-$^{18}O(7)$ distance 1.275 Å. It is noteworthy that the

O(4)-O(5) moves to the O vacancy originally occupied by O(4) due to the physisorption. When the O(6)-O(7) axis becomes parallel to the triangle, the bond is elongated, $1.275 \rightarrow 1.426$ Å, and the molecule is bound tightly to the (111) polar surface as state C. The stabilizing energy at route $B \rightarrow C$ is -1.63 eV. The next step is the O(5)-O(6) linkage to form the bridge of four oxygen atoms in state D with the $C \rightarrow D$ energy -3.07 eV. State E is the transition state of the conversion of the surface and adsorbate O_2 molecules. The activation energy of the interconversion is calculated to be 1.30 eV. Through the reversed routes, $E \rightarrow D' \rightarrow C' \rightarrow B' \rightarrow A'$, the O(4)-O(5) has flown away as ^{16}O-^{16}O from the CaO surface. The formation of O_4-bridge intermediates of state D or D' is the driving force for the double exchange. The geometric similarity of D between RHF/STO-3G and RHF/LANL1DZ+ seems to show that STO-3G geometries are useful for present large Ca_7O_7 clusters. The energy changes including the MP (RHF/LANL1DZ+ and 122 point charges) are also examined. For the single exchange in Fig. 3(i), it is confirmed that the intermediate d is most stable. For the double exchange in Fig. 3(ii), the stability rank $C > D > E > B$ is obtained, which is somewhat different from the rank of the MP-free STO-3G, $D > E > C > B$. However, there are surely O_2 chemisorbed states needed for exchange reactions.

The different patterns of the bridging give the single and double oxygen exchange via different key intermediates. In other words, two distinct exchanges are ascribed to the morphological difference of the surface sites, i.e., the regular lattice-point arrangement of oxygen atoms of state a or the molecularlike O_2 atoms of state A. It is noteworthy that the stabilizing energy $b \rightarrow d$ via c ($-1.25 - 3.50 = -4.75$ eV), is almost equal to the energy $B \rightarrow D$ via C ($-1.63 - 3.07 = -4.70$ eV). The energetic equality at physisorbed states $\rightarrow$ intermediates leads us to the following three postulates. First, the present mechanism can be applied to peaks β and not to peak γ. Second, the observed magnitude of $R(^{16}O^{18}O)$ for peaks β_1, β_2, and β_3 is almost independent of TD temperature, which is consistent with the computational result that the O_3 intermediate for single exchange is located at a single potential minimum (d). Third, the $R(^{16}O_2)$ for peaks β_4 and β_5 increases with desorption temperature. This fact may be ascribed to the presence of the energy barrier ($D \rightarrow E$) for the double exchange in these peaks.

[1]R. V. Siriwardane, J. Colloid Interf. Sci. 116, 463 (1987).

[2]R. Spinicci, Catal. Today 4, 311 (1989).

[3]J. Cunningham and C. P. Healy, J. Chem. Soc. Faraday Trans. I 83, 2973 (1987).

[4]Y. Yanagisawa et al., Surf. Sci. 242, 513 (1991).

[5]S. Coluccia et al., J. Chem. Soc. Faraday Trans. I 78, 2111 (1982).

[6]GAUSSIAN 90, revision F, M. J. Frisch, M. Head-Gordon, G. W. Trucks, J. B. Foresman, H. B. Schlegel, K. Raghavachari, M. A. Robb, J. S. Binkley, C. Gonzalez, D. J. DeFrees, D. J. Fox, R. A. Whiteside, R. Seeger, C. F. Melius, J. Baker, R. L. Martin, L. R. Kahn, J. J. P. Stewart, S. Topiol, and J. A. Pople, Gaussian, Inc., Pittsburgh, PA, 1990.

[7]E. A. Colbourn, Surf. Sci. Rep. 15, 281 (1992), and references therein.

[8]D. Stromberg, Surf. Sci. 275, 473 (1992).

[9]P. J. Hay and W. R. Wadt, J. Chem. Phys. 82, 270 (1985); W. R. Wadt and P. J. Hay, ibid. 82, 284 (1985); P. J. Hay and W. R. Wadt, ibid. 82, 299 (1985).

[10]T. Clark et al., J. Comp. Chem. 4, 294 (1983).

[11]M. M. Freund et al., Phys. Rev. Lett. 63, 2096 (1989).